Title: Towards a resolution of conflicting models of illusory contour processing in humans.

Authors: Knebel JF, Murray MM

Journal: NeuroImage

Year: 2012 Feb 1

Issue: 59

Volume: 3

Pages: 2808-17

DOI: 10.1016/j.neuroimage.2011.09.031

Towards a resolution of conflicting models of illusory contour processing in humans

Jean-François Knebel[1,2] and Micah M. Murray[1,2,3]

The Functional Electrical Neuroimaging Laboratory,
[1]Neuropsychology and Neurorehabilitation Service, Department of Clinical Neurosciences,
[2]Radiology Department
Vaudois University Hospital Center and University of Lausanne, 1011 Lausanne, Switzerland
[3]EEG Brain Mapping Core, Center for Biomedical Imaging, 1011 Lausanne, Switzerland

***Address correspondence to:**
Micah M. Murray (micah.murray@chuv.ch)
EEG Brain Mapping Core,
CIBM, Radiology, BH08.078
CHUV, Rue du Bugnon 46
1011 Lausanne, Switzerland

Manuscript information
Abbreviated title: Illusory contour processing in humans
Number of text pages: 23
Number of tables: 0
Number of figures: 6; 2 grayscale and 4 color

Abstract

Despite myriad studies, neurophysiologic mechanisms mediating illusory contour (IC) sensitivity remain controversial. Among the competing models one favors feed-forward effects within lower-tier cortices (V1/V2). Another situates IC sensitivity first within higher-tier cortices, principally lateral-occipital cortices (LOC), with later feedback effects in V1/V2. Still others postulate that LOC are sensitive to salient regions demarcated by the inducing stimuli, whereas V1/V2 effects specifically support IC sensitivity. We resolved these discordances by using misaligned line gratings, oriented either horizontally or vertically, to induce ICs. Line orientation provides an established assay of V1/V2 modulations independently of IC presence, and gratings lack salient regions. Electrical neuroimaging analyses of visual evoked potentials (VEPs) disambiguated the relative timing and localization of IC sensitivity with respect to that for grating orientation. Millisecond-by-millisecond analyses of VEPs and distributed source estimations revealed a main effect of grating orientation beginning at 65ms post-stimulus onset within the calcarine sulcus that was followed by a main effect of IC presence beginning at 85ms post-stimulus onset within the LOC. There was no evidence for differential processing of ICs as a function of the orientation of the grating. These results support models wherein IC sensitivity occurs first within the LOC.

Keywords: event-related potential; ERP; perceptual filling-in; subjective completion; object recognition, visual evoked potential; VEP

1. Introduction

Object recognition is possible despite degraded visual conditions and impediments that produce discontinuous or absent boundaries within or between objects. Experimentally, stimuli producing illusory contours (ICs) have been used to mimic these conditions (Figure 1). Despite extensive research in humans and animals, controversy persists regarding the neurophysiologic mechanisms of IC sensitivity and IC perception (Seghier and Vuilleumier, 2006).

Three general models vary according to the region considered critical for discriminating illusory contours (Figure 2). One favors a predominant role of lower-tier cortices (V1/V2) through feed-forward and/or intrinsic long-range horizontal interactions (von der Heydt and Peterhans, 1989; Peterhans and von der Heydt, 1989; Grosof et al., 1993; Ffytche and Zeki, 1996; Sheth et al., 1996; Ramsden et al., 2001). Another favors higher-tier cortices, principally lateral-occipital cortex (LOC), as being the first to exhibit sensitivity to the presence of ICs (Mendola et al., 1999; Kruggel et al., 2001; Pegna et al., 2002; Murray et al., 2002, 2004, 2006; Halgren et al., 2003; Brighina et al., 2003; Foxe et al., 2005; Brodeur et al., 2008; de-Wit et al., 2009; also Lee and Nguyen, 2001; Sáry et al., 2007, 2008). Still others postulate that the effects within LOC reflect sensitivity to so-called "salient regions" demarcated by the inducing stimuli and containing surface information, but nonetheless lacking the bounding contours of illusory contours (cf. Figure 1 in Shpaner et al., 2009). According to this model, LOC first performs crude region-based segmentation, followed by subsequent illusory contour sensitivity in V1/V2 (Stanley and Rubin, 2003; Yoshino et al., 2006; though see Shpaner et al., 2009). This model can thus be considered something of a compromise between the above models, except that no provision is made for illusory contours that lack salient regions as in the case of misaligned abutting gratings.

Distinctions between these models can thus be achieved by on the one hand considering both the locus and timing of illusory contour sensitivity and on the other hand a careful selection of stimuli, particularly for non-invasive studies in humans. Electroencephalographic (EEG) and magneto-encephalographic (MEG) recordings reliably demonstrate effects within LOC at ~100-150ms post-stimulus onset (Murray et al., 2002, 2004, 2006; Shpaner et al., 2009; Knebel et al., 2011; see also Kruggel et al., 2001; Halgren et al., 2003; Ritzl et al., 2003; Kometer et al., 2011), but have generally failed to document

early-latency effects within V1/V2 (but see Abu Bakar et al., 2008 for short-duration effects estimated within V1/V2); though embracing the null hypothesis remains problematic, despite this negative result having been replicated by independent experiments/laboratories. Late latency (presumably feedback) modulations in V1/V2 have been reported based on visual evoked fields (VEFs) from MEG (Ohtani et al., 2002; Halgren et al., 2003). In the case of hemodynamic imaging, evidence for IC sensitivity within V1/V2 is similarly unreliable. Some report robust effects (Hirsch et al., 1995; Larsson et al., 1999; Seghier et al., 2000; Maertens and Pollmann, 2005; Montaser-Kouhsari et al., 2007), others none (Kruggel et al., 2001; Murray et al., 2002; Stanley and Rubin, 2003), and still others observed V1/V2 modulations with abutting gratings but significantly less so with Kanizsa-type stimuli (Mendola et al., 1999).

Another contributing factor is therefore the choice of stimuli. Investigations in animals and humans suggest that misaligned gratings elicit larger response modulations than Kanizsa-type stimuli (Peterhans and von der Heydt, 1989; von der Heydt and Peterhans, 1989; Mendola et al., 1999). However, this appears to depend on the specific region under investigation. Mendola et al. (1999) only observed larger effects for misaligned abutting gratings within lower-tier visual cortices, whereas equivalent effects across inducer varieties were observed in higher-tier regions (see also Montaser-Kouhsari et al., 2007). Thus, misaligned abutting gratings may be particularly well-suited for studying the contribution of V1/V2 to illusory contour sensitivity; something upon which the present study sought to capitalize. Psychophysical data in humans likewise indicate there to be perceptual differences between types of illusory contours (Li and Guo, 1995; Gurnsey et al., 1996) and as a function of stimulus features in the case of abutting gratings (Soriano et al., 1995). Of pertinence to the present study, the strongest perceptions were reported when the gratings were oriented either vertically or horizontally vs. obliquely (i.e. with the corresponding illusory contour being oriented horizontally and vertically, respectively) and when the inter-line spacing of the grating was less than ~1° (Soriano et al., 1995; see also Mendola et al., 1999 for corresponding fMRI evidence). Single-unit studies, by contrast, indicate there to be a mixed population of neurons (at least within V2), such that some show invariant responsiveness as a function of grating's spatial frequency and others a return to spontaneous activity levels for inter-line spacing above ~1° (cf. Figure 15 in von der Heydt and Peterhans, 1989; see also Nieder and Wagner 1999 for evidence in owl visual Wulst for

response invariance across spatial frequency changes). Thus, grating orientation but not necessarily the spatial frequency of the grating, may be an informative low-level visual feature that can be independently varied with the presence vs. absence of illusory contours.

From a neurophysiologic standpoint, using abutting gratings to induce illusory contours is advantageous insofar as line orientation reliably modulates lower-tier visual cortices, including V1/V2, in a bottom-up manner (e.g. Sheth et al., 1996; Shapley, 2007). When orientation tuning is considered alongside evidence of anisotropic representations of orientation as manifested in the so-called oblique effect (e.g. Zemon et al., 1983; Furmanski and Engel, 2000) as well as radial biases in orientation sensitivity (e.g. Sasaki et al., 2006), it becomes theoretically possible to use differential responses to grating orientation as an independent metric of V1/V2 responsiveness from illusory contour sensitivity. This is indeed supported by demonstrations of differential responsiveness to vertical vs. horizontal gratings within lower-tier retinotopic visual cortices, including V1/V2 (Yacoub et al., 2008; Mannion et al., 2010a,b; Aspell et al., 2010; see also Ng et al., 2010 for evidence from the pigeon visual Wulst), as well as at early post-stimulus latencies (~80ms post-stimulus; Zemon et al., 1983; Moskowitz and Sokol, 1985; Koelewijn et al., 2011). By applying electrical neuroimaging analyses of visual evoked potentials (VEPs; (Murray et al., 2008) in combination with a 2x2 within subject design that varied grating orientation and IC presence, we were able to determine the timing, locus, and independence of orientation sensitivity and IC sensitivity. We reasoned that orientation sensitivity should provide a robust metric of early-latency V1/V2 modulations against which to juxtapose the timing and localization of IC sensitivity.

2. Materials and Methods

2.1. Participants

A total of 18 individuals participated (9 males; 1 left-handed) in this study, aged 20-34 years at the time of EEG recording. No participant had a history of or current neurological or psychiatric illness. All had normal or corrected-to-normal vision. Data from 3 participants were excluded due to poor EEG signal quality. The presented analyses are therefore based on a final population of 15 subjects (7 males; 1 left-handed), aged 20-34.

2.2. Stimuli and Task

The stimuli were composed of vertical and horizontal line gratings of 3 different spatial frequencies (1, 2 and 3 cycles per degree) that appeared white on a black background (i.e. 100% contrast). These were the no contour (NC) stimuli (see Figure 1). The IC stimuli were created by misaligning the gratings by half a cycle (i.e. 180° phase offset). There were 2 possible shapes – a circle and a diamond. When present, the shapes subtended 6° of visual angle. There were thus a total of 18 physically distinct stimuli, and the presentation of an IC stimulus was twice as likely as that of an NC stimulus (we return to this when discussing the analyses of the VEPs). The spatial frequency, grating orientation, and induced shape were varied to minimize adaptation effects across trials (Montaser-Kouhsari et al., 2007) as well as to reduce monotony or predictability in the stimuli despite the task entailing passive viewing. The reader should note that the main analyses were based on a 2x2 within subject design, involving factors of stimulus condition (IC vs. NC) and orientation of the gratings (horizontal vs. vertical). We excluded the factor of spatial frequency for several reasons. First, it would not be readily possible to interpret any main effect of spatial frequency with these particular stimuli because changes in spatial frequency were coupled with the number of pixels in the stimulus (and hence its physical energy). Second, including spatial frequency as a third factor in our analyses would have greatly diminished the signal quality of the VEPs because of the inclusion of fewer epochs. Third, VEP studies of spatial frequencies similar to those used in the present study (irrespective of the presence/absence of illusory contours) have shown effects at ~90ms that are localized (using equivalent current dipole modeling) to more lateral occipital cortices (cf. Figure 2 of Melis et al., 2008; Kinemans et al., 2000). By contrast, early-latency responses to higher spatial frequencies (i.e. >4 cycles per degree) result in effects within more medial occipital cortices, consistent with V1/V2 (Melis et al., 2008; Proverbio et al., 2010). Thus, it is difficult to unequivocally associate VEP modulations as a function of spatial frequency to effects within V1/V2; something critical for the present assessment of models of illusory contour sensitivity. Last and most critically, the literature provides ambiguous predictions regarding the role of spatial frequency in illusory contour sensitivity. On the one hand, single-unit studies in monkeys (von der Heydt and Peterhans, 1989) and owls (Nieder and Wagner, 1999) indicate that response modulations to illusory contours are invariant to changes in spatial frequency (though effects of the absolute number of lines have been reported). On the other hand, studies in humans provide evidence that spatial frequency can interact with the subjective strength of IC perception

(Soriano et al., 1995) and BOLD response modulations within higher-tier LOC (Mendola et al., 1999).

The stimuli were presented within the context of an interposed auditory experiment that required participants to discriminate human vocalizations from other sound sources (Aeschlimann et al., in preparation). No task was required with the visual stimuli (note that prior studies from our group have shown nearly identical effects with Kanizsa-type stimuli under active and passive conditions; Murray et al., 2002, see also Mendola et al., 1999 for results following passive stimulus viewing). Participants were instructed to fixate a centrally presented crosshair and to avoid blinking during stimulus presentations. Visual stimuli were presented for 200ms. The inter-stimulus interval (ISI) between the end of the sound (2s duration) and the visual stimuli (ISI1) varied from 500ms to 900ms. The ISI between the end of the visual stimuli (ISI2) and the next sound varied according to the equation (ISI2=1400ms – ISI1; ISI2 ϵ [500; 900ms]). The order of visual stimuli within a block of trials stimuli was randomized, but each stimulus appeared 8 times within each block. Stimulus delivery and response recordings were controlled by E-Prime (Psychology Software Tools Inc., Pittsburgh, USA; www.pstnet.com/eprime). Stimuli were presented on a 21" CRT monitor at a viewing distance of 100cm from the participant.

2.3. EEG acquisition and pre-processing

Continuous EEG was acquired at 1024Hz through a 160-channel Biosemi ActiveTwo AD-box (http://www.biosemi.com) referenced to the common mode sense (CMS; active electrode) and grounded to the driven right leg (DRL; passive electrode), which functions as a feedback loop driving the average potential across the electrode montage to the amplifier zero (full details, including a diagram of this circuitry, can be found at http://www.biosemi.com/faq/cms&drl.htm).

EEG epochs were time-locked to the presentation of visual stimuli and spanned 100ms pre-stimulus and 500ms post-stimulus. Epochs with amplitude deviations in excess of ±80µV at any channel, with the exception of those labeled as 'bad' due to poor electrode-skin contact or damage, were considered artifacts and were excluded. Likewise, trials with blinks or other transients were excluded off-line based on vertical and horizontal electrooculograms. Data from 'bad' channels were interpolated using 3D splines (Perrin et al.

1987). Prior to group-averaging VEPs, data were band-pass filtered (0.1-60Hz), re-calculated to an average reference, and baseline corrected using the pre-stimulus interval.

For the 2x2 analysis involving factors of stimulus condition (IC vs. NC) and stimulus orientation (horizontal vs. vertical gratings), 6 VEPs were calculated for each participant that were each based on the acceptance of ~200 epochs (average across subject; range: 202-206; 1-way ANOVA: $F_{(5,70)}$=28.8, p=0.31 based on an analysis that included separate tallies as a function of induced shape). There were three stimulus varieties (NC, IC when forming a diamond, and IC when forming a circle) and two grating orientations (horizontal and vertical). Because preliminary VEP analyses failed to reveal differences between IC conditions that formed a diamond vs. circle, we collapsed these data in subsequent analyses by repeating the entry of the NC condition in the ANOVA.

2.4. EEG analyses

The analyses were performed using the Cartool software programmed by Denis Brunet (http://sites.google.com/site/fbmlab/cartool/cartooldownload; Brunet et al., 2011). Effects were identified with an analysis procedure, referred to as electrical neuroimaging, which quantifies reference-independent global measures of the electric field at the scalp as well as distributed source estimations (Michel et al., 2004; Murray et al., 2008). Because our previous investigations have reliably demonstrated that IC sensitivity stems from modulations in response strength and not response topography (Murray et al., 2004, 2006; Foxe et al., 2005; Shpaner et al., 2009), we focused our analyses of the electric field at the scalp on the quantification of global field power (GFP; Lehmann and Skrandies, 1980). GFP equals the spatial standard deviation across the electrode montage and yields larger values for stronger responses (Koenig and Melie-García, 2010). GFP values at each time point were compared with a repeated measures ANOVA. To account for temporal auto-correlation, only effects ($p<0.05$) persisting for at least 11 time frames (>10ms) were considered reliable (Guthrie and Buchwald, 1991). Nonetheless, to ensure that we did not overlook topographic modulations in the present dataset, we also conducted a time point by time point analysis of global dissimilarity (Wirth et al., 2008; Koenig et al., 2011). As no statistically reliable effects were observed, we do not discuss global dissimilarity in the Results section.

In addition, we estimated the intracranial sources of the VEPs as a function of time using a distributed linear inverse solution (ELECTRA) and applying the local autoregressive

average (LAURA) regularization approach to address the non-uniqueness of the inverse problem (Grave de Peralta Menendez et al., 2001, 2004; Michel et al., 2004). The inverse solution algorithm is based on biophysical principles derived from the quasi-static Maxwell's equations; most notably the fact that independent of the volume conductor model used to describe the head, only irrotational and not solenoidal currents contribute to the EEG (Grave de Peralta Menendez et al., 2001, 2004). As part of the regularization strategy, homogenous regression coefficients in all directions and within the whole solution space were used. LAURA uses a realistic head model, and the solution space included 3005 nodes, selected from a 6 × 6 × 6mm grid equally distributed within the gray matter of the Montreal Neurological Institute's average brain (courtesy of Grave de Peralta Menendez and Gonzalez Andino; http://www.electrical-neuroimaging.ch/). The head model and lead field matrix were generated with the Spherical Model with Anatomical Constraints (SMAC;Spinelli et al., 2000). As an output, LAURA provides current density measures; the scalar values of which were evaluated at each node. Prior basic and clinical research has documented and discussed in detail the spatial accuracy of this inverse solution (e.g.Grave de Peralta Menendez et al., 2004; Michel et al., 2004; Gonzalez Andino, Michel, et al., 2005; Gonzalez Andino, Murray, et al., 2005; Martuzzi et al., 2009). The source estimations were calculated for each time point, subject and condition. These data matrices were then submitted to a repeated measures ANOVA as a function of time (see also Britz and Michel, 2010). To partially correct for multiple testing and temporal auto-correlation we applied an significance threshold of $p<0.01$, a temporal criterion of 11 consecutive time-frames, and a spatial extent criterion of 15 contiguous solution points (see also De Lucia et al., 2010 for a similar approach).

3. Results

We would remind the reader that the subjects passively viewed the visual stimuli while centrally fixating (i.e. subjects were performing a task on intervening sounds). As such, there are no behavioral results to report, though prior work has shown near-ceiling performance when discriminating the presence vs. absence of Kanizsa-type illusory contours and nearly identical VEP modulations for active vs. passive viewing conditions (e.g. Murray et al., 2002).

A first level of analysis of the VEP was performed using individual voltage waveforms, though we would remind the reader that our conclusions were based on reference-independent measures. VEPs from an occipital midline electrode (OZ) and a parieto-occipital electrode (PO6) are shown in Figure 3. Visual inspection of these waveforms was suggestive of two stages of differential responses: first an orientation differentiation (~60ms) followed by a modulation as a function of IC presence vs. absence (~100ms). These observations were statistically evaluated via a time-point by time-point 2x2 repeated measures ANOVA. There was a main effect of stimulus orientation (63-74ms at Oz and 74-112ms and 209-297ms at PO6). There was also a main effect of stimulus condition (228-291ms and 355-387ms for Oz and 107-143ms and 241-291ms for PO6). There was no evidence for an interaction at any latency.

As described in the Materials and Methods, the VEP data were analyzed using electrical neuroimaging methods; here principally in terms of reference-independent GFP waveforms. Group-averaged GFP waveforms from each condition are displayed in Figure 4. As above, Visual inspection of these waveforms suggests there to be differences as a function of stimulus orientation followed by effects of stimulus condition. These millisecond-wise 2x2 ANOVA on the GFP revealed a main effect of stimulus orientation over the 65-107ms, 128-175ms and 365-400ms post-stimulus intervals. Responses over the initial ~100ms were generally stronger responses to the 'vertical' than 'horizontal' condition (Maffei and Campbell, 1970). There was also a main effect of stimulus condition over the 85-102ms and 371-387ms post-stimulus intervals, with generally stronger responses to IC than NC stimuli. There was no evidence for an interaction at any latency.

Given the above GFP results, the analyses of the source estimations focused on the initial 200ms post-stimulus interval, but were nonetheless carried out over the 400ms post-stimulus period. The repeated measures ANOVA revealed a main effect of stimulus orientation over the ~60-90ms post-stimulus period that was located in bilateral occipital and temporal regions, including the calcarine sulcus, with stronger responses to vertical than horizontal stimuli (Figure 5; green traces). A visualization of the distribution of this main effect is displayed at 66ms post-stimulus onset (green-framed inset in Figure 5). There was a main effect of stimulus condition over the ~80-130ms post-stimulus period that was located first within left temporo-parietal regions (~80-110ms) and subsequently within right temporo-parietal regions (~100-130ms; Figure 5, orange traces and orange-framed inset).

Source estimations were stronger for IC than NC stimuli. These regions extended along a dorsal-ventral axis to include lateral occipital cortices (cf. Table 3 in Grill-Spector et al., 1998). Finally and in general agreement with evidence from MEG for IC sensitivity within the occipital pole (and presumably V1/V2) at relatively late post-stimulus latencies (Halgren et al., 2003), we also observed a main effect of stimulus condition over the ~280-340ms post-stimulus period that included effects within the calcarine sulcus as well as lateral and inferior occipito-temporal cortices (Figure 6).

4. Discussion

The present study set out to resolve discordances across extant models of IC sensitivity. To do this, we recorded VEPs in response to misaligned line gratings that in turn induced the perception of illusory contour shapes. Moreover, by varying the orientation of these gratings (both when inducing an IC and not), we could assay responsiveness of low-level visual cortices. The application of electrical neuroimaging analyses to these VEPs allowed us to determine both the temporal and spatial dynamics of IC sensitivity relative to that for grating orientation. We show that sensitivity to grating orientation transpires over the 60-90ms post-stimulus interval, principally within the calcarine sulcus, and prior to IC sensitivity over the 80-110ms post-stimulus interval, principally within the LOC (though later effects were observed within V1/V2). There was no evidence for interactions between the sensitivity to each of these features. As such, the collective data provide further support to models of IC sensitivity within the LOC that in turn mediates subsequent effects within V1/V2 (see also Dura-Bernal et al., 2011 for recent computational modeling of IC sensitivity).

One major advance of the present study is that the illusory contours induced by line grating stimuli on the one hand provided an IC vs. NC contrast that reliably modulates responses within V1/V2 both when examined using fMRI in humans (Mendola et al., 1999) and when recording from single neurons in animals (e.g. von der Heydt and Peterhans, 1989; Nieder and Wagner, 1999), and on the other hand controlled for the presence of salient regions in the stimuli (this latter point is discussed in detail below). Analyses both at the level of surface VEPs and estimations of intracranial sources indicate that sensitivity to grating orientation, independent of the induction of illusory contours, occurred during the initial stages of visual processing (60-90ms) within regions within the calcarine sulcus and

surrounding cortices. This effect coincides with the C1 component of the VEP, which is known to include prominent generators within V1/V2 (Clark et al., 1995; Foxe et al., 2008). This effect of orientation sensitivity was followed by IC sensitivity (80-110ms) within the LOC and extended dorsally into parietal regions (though excluding modulations at this latency within the calcarine sulcus; Figure 5). This effect of IC sensitivity was likewise independent of grating orientation. Subsequent stages of IC sensitivity (~280-340ms), however, indeed demonstrated effects within the calcarine sulcus (and likely V1/V2; see also Halgren et al., 2003). Additionally, the high temporal resolution of electrical neuroimaging allowed us to situate IC sensitivity in time and space with respect to these modulations within V1/V2. This collective pattern demonstrates the appropriateness of the stimuli as well as the sensitivity of our electrical neuroimaging methods to produce reliable effects within lower-tier visual cortices. However, we would acknowledge that despite using 160-channel VEPs and being able to detect modulations in GFP, we were unable to document statistically reliable topographic (and therefore generator configuration) differences between the horizontal and vertical orientations, which would constitute evidence for the sensitivity of surface-recorded VEPs to the differential activity of sub-populations of neurons (e.g. orientation columns) within lower-tier visual cortices (see e.g. Yacoub et al., 2008 for such evidence based on fMRI at 7 Tesla). This sensitivity awaits further advances in EEG/MEG acquisition and analysis methods.

That IC sensitivity occurs first within the LOC is highly consistent with prior VEP results using Kanizsa-type stimuli. In a series of studies by our group (Pegna et al., 2002; Murray et al., 2002, 2004, 2006; Foxe et al., 2005; Shpaner et al., 2009; Knebel et al., 2011) it was shown that IC sensitivity onsets ~90ms post-stimulus within LOC irrespective of contrast polarity, modal vs. amodal completion, active vs. passive viewing, and accuracy during IC curvature discrimination (see also Brodeur et al., 2008). In all cases, IC sensitivity manifested as a modulation in response strength (i.e. GFP) with no evidence for topographic differences relative to the NC condition. Parsimony thus favors a mechanism whereby a configuration of statistically indistinguishable intracranial generators responds more strongly to IC presence than absence, which was further confirmed by source estimations in these studies. This pattern accords with findings at the single-cell level in animals (Lee and Nguyen, 2001; Sáry et al., 2007), as well as with MEG recordings (Halgren et al., 2003) and functional magnetic

resonance imaging (fMRI) investigations in humans (Mendola et al., 1999; Kruggel et al., 2001).

The present findings extend this pattern to show that misaligned line gratings elicit qualitatively similar effects as Kanizsa-type stimuli in their timing, directionality, and localization. Using MEG, Ohtani et al. (2002) described IC sensitivity based on misaligned line gratings that manifested as stronger responses to IC than NC conditions over the 80-150ms post-stimulus period, which followed overall MEG response onset by 20-30ms. However, effects were only reliable in just two of their four subjects. In their seminal fMRI study, Mendola et al. (1999) found larger effects of IC sensitivity induced by misaligned gratings than by Kanizsa-type stimuli (additional conditions included stereopsis-defined and luminance-defined shapes). It will therefore be of interest for future research or meta-analyses to establish a quantitative metric of IC sensitivity for different varieties of inducers based on EEG data. More recently, Montaser-Kouhsari et al. (2007) examined the impact of grating orientation on adaptation to ICs as measured with fMRI from four observers. While they observed orientation-sensitive adaptation effects throughout visual cortices, they were larger within higher-tier than lower-tier regions. This increase across regions was furthermore not readily explained by passive transmission of effects (perhaps in a bottom-up fashion) from lower-tier to higher-tier regions. Instead, they leave open the possibility that IC sensitivity and its adaption may originate within higher-tier regions, including LOC, and acknowledge the need for measurements with higher temporal resolution. The present electrical neuroimaging study provides this temporal information as well as a reasonable degree of spatial localization. While we were not able to detect any interactions between IC sensitivity and orientation sensitivity here, applying an adaptation paradigm similar to that in Montaser-Kouhsari et al. (2007), a wider range of orientations and spatial frequencies, and/or other task parameters explicitly requiring attention to stimulus orientation may uncover finer levels of interaction between contour and orientation processes. Such notwithstanding, the present findings do indicate a degree of successive processing of orientation information first within lower-tier visual cortices and subsequently contour information within higher-tier visual cortices.

While the present data clearly support a model of IC sensitivity wherein effects within lower-tier visual cortices (V1/V2) are driven by feedback activity from the LOC (and perhaps also elsewhere), it could still be contended that it is salient regions of the stimuli rather than

illusory contours per se that are being treated within the LOC and that sensitivity to the ICs themselves is a function specific to V1/V2 (see Model 3 in Figure 2). This model was initially put forward by Stanely and Rubin (2003) based on fMRI results showing equivalent depth of modulation within the LOC to Kanizsa-type ICs as well as rounded versions of these stimuli that lacked a perception of bound contours, but nonetheless demarcated a rough surface. It is worth noting, however, that while their model proposes a differential response within V1/V2 to ICs versus these rounded versions, their actual data provide no direct evidence for such. Other empirical data examining the effect of distracter inducer arrays on the detection of Kanizsa-type illusory contour targets have shown that the progressive presence of a distracter illusory figure (i.e. due to incrementally aligning the mouths of the "pacmen" inducers) affected late-latency ERP responses (>200ms post-stimulus onset; Conci et al., 2006). Such data are incompatible with Model 3 in Figure 2, because the progressive apparition of illusory figures would be predicted to modulate ERPs during earlier time periods consistently documented to be sensitive to the presence vs. absence of ICs (i.e. ~100-150ms post-stimulus onset; see also Scholte et al., 2008). Similarly incompatible with Model 3 are ERP data from Herrmann and Bosch (2001) wherein larger responses over the 150-180ms post-stimulus period were obtained for Kanizsa-type IC stimuli relative to a number of control stimuli, including one inducing collinear illusory borders in the absence of an illusory form and associated Gestalt perception. Importantly, all stimuli in their study included the same number of collinear inducer lines. Thus, it is unlikely that salient region processing or surface segmentation is the principal cause of these ERP modulations. More recently, Shpaner et al. (2009) conducted an electrical neuroimaging study with similar stimuli to those used by Stanley and Rubin (2003) in their fMRI study so as to directly assess this model and its inherent temporal predictions. They found that initial responses within the LOC were significantly stronger for IC stimuli than to rounded versions of the stimuli and also differed topographically. Because topographic differences must follow from changes in the configuration of intracranial generators (discussed in Murray et al., 2008), the processing of IC stimuli and salient region stimuli must rely on at least partially distinct brain networks. Source estimations performed by Shpaner et al. (2009) indeed indicate that that while illusory contour/form stimuli resulted in significant modulations (relative to the no contour control condition) in LOC, this was not the case at this latency in response to salient region stimuli (cf. Figure 5 of Shpaner et al., 2009). Thus, initial responsiveness within the LOC

cannot simply reflect the discrimination of salient regions within the visual scene. However, as neither of these studies reported evidence for IC sensitivity (early or late) within V1/V2, it is impossible from these data alone to completely dismiss other models proposing feedforward IC sensitivity within V1/V2 (cf. Model 1 in Figure 2). Likewise, neither of these studies provided evidence for V1/V2 responsiveness to another stimulus parameter against which they could situate the timing of (and/or magnitude in the case of fMRI) IC sensitivity. Instead, data from Mendola et al. (1999) speak to this issue by showing stronger IC effects within the LOC and other higher-tier visual cortices with stimuli with lower spatial frequencies (and by extension fewer line endings that could arguably be said to provide progressively less information concerning salient regions in the image; cf. their Figure 6). It is worth noting, however, that their manipulation of spatial frequency did not affect IC sensitivity within retinotopic cortices, including V1/V2. This pattern is consistent with some single-neuron recordings within area V2 of monkeys (von der Heydt and Peterhans, 1989) and the visual Wulst of owls (Nieder and Wagner, 1999) showing invariance of IC sensitivity to manipulations of gratings' spatial frequency. Such data notwithstanding, it will be crucial for future research to conduct appropriate experiments to unequivocally distinguish between Models 2 and 3 as represented in Figure 2. Among several ways forward would be to parametrically vary the number of illusory borders induced (thereby affecting the presence/absence of a perceived form) or alternatively the spatial frequency of the line gratings (while also controlling for the overall luminance of and lines present in the inducers). In our view, such paradigms should be combined with electrical neuroimaging as well as transcranial magnetic stimulation to facilitate causal inferences on the role of specific brain regions at specific post-stimulus latencies (e.g. Thut and Pascual-Leone 2010a,b; Ilmoniemi and Kicic, 2010; Johnson et al., 2010; Miniussi and Thut, 2010; Zanon et al. 2010). In parallel, recent efforts in computational modeling support the role of feedback modulations from a layer resembling the properties of LOC (Dura-Bernal et al., 2011). While this model was able to detect illusory contours and forms with classical Kaniza-type stimuli, it performed unsuccessfully when confronted with blurred inducers akin to those used by Stanley and Rubin (2003) to induce salient regions (cf. Figure 5 in Dura-Bernal et al., 2011). Such modeling results support the notion that IC sensitivity precedes and may be partially independent of surface segmentation.

Despite the evidence presented in the current and our prior works (Murray et al., 2002, 2004, 2006; Pegna et al., 2002; Foxe et al., 2005; Shpaner et al., 2009; Knebel et al., 2011), as well as those from other independent laboratories (e.g. Herrmann and Bosch, 2001; Kruggel et al. 2001; Ohtani et al., 2002; Halgren et al., 2003), it may nonetheless be contended that IC sensitivity within V1/V2 is sufficiently "small" in its magnitude or number of recruited neurons and/or involves a configuration of local generators that obfuscates its propagation to the scalp and thus its detection using either VEPs or VEFs (see also Ramsden et al., 2001 for evidence of oppositely signed effects in response to illusory contours in V1 and V2). By this line of reasoning, Model 1 in Figure 2 would account for IC sensitivity, and our embracing of Model 2 would be erroneous.

In this regard, it is worth noting that about half of the neurons recorded in V1 (Grosof et al., 1993) or V2 (von der Heydt and Peterhans, 1989) of macaques exhibited IC sensitivity and that the magnitude of spiking activity of these neurons was roughly equal to and sometimes greater than that observed upon presentation of a luminance-defined line (e.g. von der Heydt and Peterhans, 1989; Lee and Nguyen, 2001; though see Nieder and Wagner, 1999). Such data would suggest that a detectable response reflecting IC sensitivity should likely appear in scalp-recorded VEPs and VEFs from humans. Regarding the possibility that IC sensitivity in V1/V2 is masked by other, stronger activity co-occurring elsewhere, fMRI studies report IC sensitivity within V1/V2 that is of similar magnitude as that in other higher-tier visual cortices (Mendola et al., 1999; Seghier et al., 2000; Montaser-Kouhsari et al., 2007). Accordingly, we would highlight the statistically robust IC sensitivity in V1/V2 at ~300ms post-stimulus onset observed in the present study (see Figure 6) as well as in prior VEF studies (Halgren et al., 2003).

Such notwithstanding, it is therefore of critical importance to consider the latency of any IC sensitivity within V1/V2 and to situate such relative to general response onset and sensitivity to other stimulus features. The present study and our collective prior works would indicate there to be an approximate 40-50ms lag between VEP onset and the onset of statistically robust IC sensitivity. This is in strong agreement with studies in animals that considered the timing of their effects. Lee and Nguyen (2001) examined the latency and laminar distribution of IC sensitivity in areas V1 and V2. They found the earliest effects at 70ms within supragranular layers of area V2, consistent with a feedback profile (cf. their Figure 4; see also Sary et al. 2007 for a similar consideration of timing of IC sensitivity within

infero-temporal regions). With regard to sensitivity to other stimulus features, our prior work has shown there to be sensitivity to the spatial distribution of Kanizsa-type inducers over the ~55-90ms post-stimulus period within parietal regions (Murray et al., 2002; Knebel et al., 2011) that is furthermore independent of the presence/absence of illusory contours. The present study adds to these findings by showing there to be sensitivity to grating orientation over the 60-90ms post-stimulus interval that is localized to V1/V2 and that is similarly independent of the presence/absence of illusory contours (Figure 5). As such, we consider it highly unlikely that our methods/paradigm suffer from insensitivity to early-latency effects within V1/V2. Nonetheless, it is clear that additional studies will be required to conclusively address these issues, perhaps taking advantage of developments in near-infrared spectroscopy or the possibility to record intracranially in human patients during pre-surgical epilepsy monitoring.

5. Conclusions

The present study combined an optimized stimulus with state-of-the-art analyses of scalp-recorded VEPs to provide spatio-temporal information regarding mechanisms of illusory contour sensitivity in humans. As such, we were able to disambiguate competing models generated from a combination of evidence from humans and animals. First, the initial IC sensitivity we documented was subsequent to and spatially distinct from preceding effects of grating orientation. This allowed us to invalidate models based on early, feedforward sensitivity within V1/V2 (von der Heydt and Peterhans, 1989; Peterhans and von der Heydt, 1989; Ffytche and Zeki, 1996; Ramsden et al., 2001). Second, the consistency of the present effects using line gratings with our and others' previous observations using Kanizsa-type stimuli (Herrmann and Bosch, 2001; Murray et al., 2002, 2004, 2006) allowed us to invalidate models claiming that initial responsiveness within the LOC is due to the detection of salient regions that in turn drive IC sensitivity within V1/V2. Instead, the collective results support models wherein IC sensitivity occurs first within the LOC.

Acknowledgements

This work has been supported by the Swiss National Science Foundation (grants 310030B_133136 and 320000_120579 as well as the National Center of Competence in Research project "SYNAPSY — The Synaptic Bases of Mental Disease"; project no. 51AU40_125759). The Cartool software has been programmed by Denis Brunet, from the Functional Brain Mapping Laboratory, Geneva, Switzerland, and is supported by the EEG Brain Mapping Core of the Center for Biomedical Imaging (www.cibm.ch) of Geneva and Lausanne. It is freely available at: http://sites.google.com/site/fbmlab/cartool/cartooldownload. We thank Laurent Udry and Melanie Aeschlimann for their assistance during data collection.

References

Abu Bakar, A., Liu, L., Conci, M., Elliott, M.A., Ioannides, A.A., 2008. Visual field and task influence illusory figure responses. Human Brain Mapping 29, 1313-1326.

Aspell, J.E., Wattam-Bell, J., Atkinson, J., Braddick, O.J., 2010. Differential human brain activation by vertical and horizontal global visual textures. Exp. Brain Res. 202, 669-79.

Brighina, F., Ricci, R., Piazza, A., Scalia, S., Giglia, G., Fierro, B., 2003. Illusory contours and specific regions of human extrastriate cortex: evidence from rTMS. European Journal of Neuroscience 17, 2469-2474.

Britz, J., Michel, C.M., 2010. Errors can be related to pre-stimulus differences in ERP topography and their concomitant sources. Neuroimage 49, 2774-2782.

Brodeur, M., Lepore, F., Lepage, M., Bacon, B.A., Jemel, B., Debruille, J.B., 2008. Alternative mode of presentation of Kanizsa figures sheds new light on the chronometry of the mechanisms underlying the perception of illusory figures. Neuropsychologia 46, 554-66.

Brunet, D., Murray, M.M., Michel, C.M., 2011. Spatiotemporal analysis of multichannel EEG: CARTOOL. Computational Intelligence and Neuroscience 2011,813870.

Clark, V., Fan, S., Hillyard, S., 1995. Identification of early visual evoked potential generators by retinotopic and topographic analyses. Human Brain Mapping 2, 170-187.

Conci, M., Gramann, K., Müller, H.J., Elliott, M.A., 2006. Electrophysiological correlates of similarity-based interference during detection of visual forms. Journal of Cognitive Neuroscience 18, 880-888.

De Lucia, M., Clarke, S., Murray, M.M., 2010. A temporal hierarchy for conspecific vocalization discrimination in humans. Journal of Neuroscience 30, 11210-11221.

de-Wit, L.H., Kentridge, R.W., Milner, A.D., 2009. Shape processing area LO and illusory contours. Perception 38, 1260-1263.

Dura-Bernal, S., Wennekers, T., Denham, S.L., 2011. The role of feedback in a hierarchical model of object perception. Adv Exp Med Biol. 718, 165-79.

Ffytche, D.H., Zeki, S., 1996. Brain activity related to the perception of illusory contours. Neuroimage 3, 104-108.

Foxe, J.J., Strugstad, E.C., Sehatpour, P., Molholm, S., Pasieka, W., Schroeder, C.E., McCourt, M.E., 2008. Parvocellular and magnocellular contributions to the initial generators of the visual evoked potential: high-density electrical mapping of the "C1" component. Brain Topography 21, 11-21.

Foxe, J.J., Murray, M.M., Javitt, D.C., 2005. Filling-in in schizophrenia: a high-density electrical mapping and source-analysis investigation of illusory contour processing. Cerebrak Cortex 15, 1914-1927.

Furmanski, C.S., Engel, S.A., 2000. An oblique effect in human primary visual cortex. Nature Neuroscience 3, 535-6.

Gonzalez Andino, S.L., Michel, C.M., Thut, G., Landis, T., Grave de Peralta, R., 2005. Prediction of response speed by anticipatory high-frequency (gamma band) oscillations in the human brain. Human Brain Mapping 24, 50-58.

Gonzalez Andino, S.L., Murray, M.M., Foxe, J.J., de Peralta Menendez, R.G., 2005. How single-trial electrical neuroimaging contributes to multisensory research. Experimental Brain Research 166, 298-304.

Grave de Peralta Menendez, R., Gonzalez Andino, S., Lantz, G., Michel, C.M., Landis, T., 2001. Noninvasive localization of electromagnetic epileptic activity. I. Method descriptions and simulations. Brain Topography 14, 131-137.

Grave de Peralta Menendez, R., Murray, M.M., Michel, C.M., Martuzzi, R., Gonzalez Andino, S.L., 2004. Electrical neuroimaging based on biophysical constraints. Neuroimage 21, 527-539.
Grill-Spector, K., Kushnir, T., Edelman, S., Itzchak, Y., Malach, R., 1998. Cue-invariant activation in object-related areas of the human occipital lobe. Neuron 21, 191-202.
Grosof, D.H., Shapley, R.M., Hawken, M.J., 1993. Macaque V1 neurons can signal 'illusory' contours. Nature 365, 550-552.
Gurnsey, R., Poirier, F.J., Gascon, E., 1996. There is no evidence that Kanizsa-type subjective contours can be detected in parallel. Perception 25, 861-74.
Guthrie, D., Buchwald, J.S., 1991. Significance testing of difference potentials. Psychophysiology 28, 240-244.
Halgren, E., Mendola, J., Chong, C.D.R., Dale, A.M., 2003. Cortical activation to illusory shapes as measured with magnetoencephalography. Neuroimage 18, 1001-1009.
von der Heydt, R., Peterhans, E., 1989. Mechanisms of contour perception in monkey visual cortex. I. Lines of pattern discontinuity. Journal of Neuroscience 9, 1731-1748.
Herrmann, C.S., Bosch, V., 2001. Gestalt perception modulates early visual processing. NeuroReport 12, 901-4.
Hirsch, J., DeLaPaz, R.L., Relkin, N.R., Victor, J., Kim, K., Li, T., Borden, P., Rubin, N., Shapley, R., 1995. Illusory contours activate specific regions in human visual cortex: evidence from functional magnetic resonance imaging. Proceedings of the National Academy of Sciences of the United States of America 92, 6469 -6473.
Ilmoniemi, R.J., Kičić, D., 2010. Methodology for combined TMS and EEG. Brain Topography 22, 233-248.
Johnson, J.S., Hamidi, M., Postle, B.R., 2010. Using EEG to explore how rTMS produces its effects on behavior. Brain Topography 22, 281-293.
Kenemans, J.L., Baas, J.M., Mangun, G.R., Lijffijt, M., Verbaten, M.N., 2000. On the processing of spatial frequencies as revealed by evoked-potential source modeling. Clinical Neurophysiology 111, 1113-23.
Knebel JF, Javitt DC, Murray MM, 2011. Impaired early visual response modulations to spatial information in chronic schizophrenia. Psychiatry Research 193, 168-176.
Koelewijn, L., Dumont, J.R., Muthukumaraswamy, S.D., Rich, A.N., Singh, K.D., 2011. Induced and evoked neural correlates of orientation selectivity in human visual cortex. Neuroimage 54, 2983-93.
Koenig, T., Melie-García, L., 2010. A method to determine the presence of averaged event-related fields using randomization tests. Brain Topography 23, 233-242.
Koenig, T., Kottlow, M., Stein, M., Melie-García, L., 2011 Ragu: a free tool for the analysis of EEG and MEG event-related scalp field data using global randomization statistics. Computational Intelligence and Neuroscience 2011, 938925.
Kometer, M., Cahn, B.R., Andel, D., Carter, O.L., Vollenweider, F.X., 2011. The 5-HT2A/1A agonist psilocybin disrupts modal object completion associated with visual hallucinations. Biological Psychiatry 69, 399-406.
Kruggel, F., Herrmann, C.S., Wiggins, C.J., von Cramon, D.Y., 2001. Hemodynamic and electroencephalographic responses to illusory figures: recording of the evoked potentials during functional MRI. Neuroimage 14, 1327-1336.
Larsson, J., Amunts, K., Gulyás, B., Malikovic, A., Zilles, K., Roland, P.E., 1999. Neuronal correlates of real and illusory contour perception: functional anatomy with PET. European Journal of Neuroscience 11, 4024-4036.

Lee, T.S., Nguyen, M., 2001. Dynamics of subjective contour formation in the early visual cortex. Proceedings of the National Academy of Sciences of the United States of America 98, 1907-1911.
Lehmann, D., Skrandies, W., 1980. Reference-free identification of components of checkerboard evoked multichannel potential fields. Electroencephalography and Clinical Neurophysiology 48, 609-621.
Li, C.Y., Guo, K., 1995. Measurements of geometric illusions, illusory contours and stereo-depth at luminance and colour contrast. Vision Research 35, 1713-20.
Maertens, M., Pollmann, S., 2005. fMRI reveals a common neural substrate of illusory and real contours in V1 after perceptual learning. Journal of Cognitive Neuroscience 17, 1553-1564.
Mannion, D.J., McDonald, J.S., Clifford, C.W., 2010a. The influence of global form on local orientation anisotropies in human visual cortex. Neuroimage 52, 600-5.
Mannion, D.J., McDonald, J.S., Clifford, C.W., 2010b. Orientation anisotropies in human visual cortex. Journal of Neurophysiology 103, 3465-71.
Martuzzi, R., Murray, M.M., Meuli, R.A., Thiran, J., Maeder, P.P., Michel, C.M., Grave de Peralta Menendez, R., Gonzalez Andino, S.L., 2009. Methods for determining frequency- and region- dependent relationships between estimated LFPs and BOLD responses in humans. Journal of Neurophysiology 101, 491-502.
Melis, C., Baas, J.M., Kenemans, J.L., Mangun, G.R., 2008. A decomposition of electrocortical activity as a function of spatial frequency: a weighted multidimensional scaling analysis. Brain Research 1214, 116-26.
Mendola, J.D., Dale, A.M., Fischl, B., Liu, A.K., Tootell, R.B., 1999. The representation of illusory and real contours in human cortical visual areas revealed by functional magnetic resonance imaging. Journal of Neuroscience 19, 8560-8572.
Michel, C.M., Murray, M.M., Lantz, G., Gonzalez, S., Spinelli, L., Grave de Peralta, R., 2004. EEG source imaging. Clinical Neurophysiology 115, 2195-2222.
Miniussi, C., Thut, G., 2010 Combining TMS and EEG offers new prospects in cognitive neuroscience. Brain Topography 22, 249-256.
Montaser-Kouhsari, L., Landy, M.S., Heeger, D.J., Larsson, J., 2007. Orientation-selective adaptation to illusory contours in human visual cortex. Journal of Neuroscience 27, 2186-2195.
Moskowitz, A., Sokol, S., 1985 Effect of stimulus orientation on the latency and amplitude of the VEP. Invest. Ophthalmol. Vis. Sci. 26, 246-8.
Murray, M.M., Brunet, D., Michel, C.M., 2008. Topographic ERP analyses: a step-by-step tutorial review. Brain Topography 20, 249-264.
Murray, M.M., Foxe, D.M., Javitt, D.C., Foxe, J.J., 2004. Setting boundaries: brain dynamics of modal and amodal illusory shape completion in humans. Journal of Neuroscience 24, 6898-6903.
Murray, M.M., Imber, M.L., Javitt, D.C., Foxe, J.J., 2006. Boundary completion is automatic and dissociable from shape discrimination. Journal of Neuroscience 26, 12043-12054.
Murray, M.M., Wylie, G.R., Higgins, B.A., Javitt, D.C., Schroeder, C.E., Foxe, J.J., 2002. The spatiotemporal dynamics of illusory contour processing: combined high-density electrical mapping, source analysis, and functional magnetic resonance imaging. Journal of Neuroscience 22, 5055-5073.

Ng, B.S., Grabska-Barwińska, A., Güntürkün, O., Jancke, D., 2010. Dominant vertical orientation processing without clustered maps: early visual brain dynamics imaged with voltage-sensitive dye in the pigeon visual Wulst. Journal of Neuroscience 30, 6713-25.

Nieder, A., Wagner, H., 1999. Perception and neuronal coding of subjective contours in the owl. Nature Neuroscienece 2, 660-3.

Ohtani, Y., Okamura, S., Shibasaki, T., Arakawa, A., Yoshida, Y., Toyama, K., Ejima, Y., 2002. Magnetic responses of human visual cortex to illusory contours. Neuroscience Letters 321, 173-176.

Pegna, A.J., Khateb, A., Murray, M.M., Landis, T., Michel, C.M., 2002. Neural processing of illusory and real contours revealed by high-density ERP mapping. Neuroreport 13, 965-968.

Peterhans, E., von der Heydt, R., 1989. Mechanisms of contour perception in monkey visual cortex. II. Contours bridging gaps. Journal of Neuroscience 9, 1749-1763.

Petry, S., Harbeck, A., Conway, J., Levey, J., 1983. Stimulus determinants of brightness and distinctness of subjective contours. Perception and Psychophysics 34, 169-174.

Proverbio, A.M., Del Zotto, M., Zani, A., 2010. Electrical neuroimaging evidence that spatial frequency-based selective attention affects V1 activity as early as 40-60 ms in humans. BMC Neuroscience 11, 59.

Ramsden, B.M., Hung, C.P., Roe, A.W., 2001. Real and illusory contour processing in area V1 of the primate: a cortical balancing act. Cereb.^ral Cortex 11, 648-665.

Ritzl, A., Marshall, J.C., Weiss, P.H., Zafiris, O., Shah, N.J., Zilles, K., Fink, G.R., 2003. Functional anatomy and differential time courses of neural processing for explicit, inferred, and illusory contours. An event-related fMRI study. Neuroimage 19, 1567-77.

Sáry, G., Chadaide, Z., Tompa, T., Köteles, K., Kovács, G., Benedek, G., 2007. Illusory shape representation in the monkey inferior temporal cortex. European Journal of Neuroscience 25, 2558-2564.

Sáry, G., Köteles, K., Kaposvári, P., Lenti, L., Csifcsák, G., Frankó, E., Benedek, G., Tompa, T., 2008. The representation of Kanizsa illusory contours in the monkey inferior temporal cortex. European Journal of Neuroscience 28, 2137-2146.

Sasaki, Y., Rajimehr, R., Kim, B.W., Ekstrom, L.B., Vanduffel, W., Tootell, R.B., 2006. The radial bias: a different slant on visual orientation sensitivity in human and nonhuman primates. Neuron 51, 661-70.

Scholte, H.S., Jolij, J., Fahrenfort, J.J., Lamme, V.A., 2008. Feedforward and recurrent processing in scene segmentation: electroencephalography and functional magnetic resonance imaging. Journal of Cognitive Neuroscience 20, 2097-2109.

Seghier, M.L., Vuilleumier, P., 2006. Functional neuroimaging findings on the human perception of illusory contours. Neuroscience and Biobehavioral Reviews 30, 595-612.

Seghier, M., Dojat, M., Delon-Martin, C., Rubin, C., Warnking, J., Segebarth, C., Bullier, J., 2000. Moving Illusory Contours Activate Primary Visual Cortex: an fMRI Study. Cerebral Cortex 10, 663 -670.

Shapley, R., 2007. Early vision is early in time. Neuron 56, 755-756.

Sheth, B.R., Sharma, J., Rao, S.C., Sur, M., 1996. Orientation maps of subjective contours in visual cortex. Science 274, 2110-2115.

Shpaner, M., Murray, M.M., Foxe, J.J., 2009. Early processing in the human lateral occipital complex is highly responsive to illusory contours but not to salient regions. European Journal of Neuroscience 30, 2018-2028.

Soriano, M., Spillmann, L., Bach, M., 1996. The abutting grating illusion. Vision Research 36, 109-16.

Spinelli, L., Andino, S.G., Lantz, G., Seeck, M., Michel, C.M., 2000. Electromagnetic inverse solutions in anatomically constrained spherical head models. Brain Topography 13, 115-125.

Stanley, D.A., Rubin, N., 2003. fMRI activation in response to illusory contours and salient regions in the human lateral occipital complex. Neuron 37, 323-331.

Thut, G., Pascual-Leone A., 2010a. Integrating TMS with EEG: How and what for? Brain Topography 22, 215-218.

Thut, G., Pascual-Leone A., 2010b. A review of combined TMS-EEG studies to characterize lasting effects of repetitive TMS and assess their usefulness in cognitive and clinical neuroscience. Brain Topography 22, 219-231.

Wirth, M., Horn, H., Koenig, T., Razafimandimby, A., Stein, M., Mueller, T., Federspiel, A., Meier, B., Dierks, T., Strik, W., 2008. The early context effect reflects activity in the temporo-prefrontal semantic system: evidence from electrical neuroimaging of abstract and concrete word reading. Neuroimage 42, 423-36.

Yacoub, E., Harel, N., Ugurbil, K., 2008. High-field fMRI unveils orientation columns in humans. Proceedings of the National Academy of Sciences of the United States of America 105, 10607-12.

Yoshino, A., Kawamoto, M., Yoshida, T., Kobayashi, N., Shigemura, J., Takahashi, Y., Nomura, S., 2006. Activation time course of responses to illusory contours and salient region: a high-density electrical mapping comparison. Brain Research 1071, 137-144.

Zanon, M., Busan, P., Monti, F., Pizzolato, G., Battaglini, P.P., 2010. Cortical Connections Between Dorsal and Ventral Visual Streams in Humans: Evidence by TMS/EEG Co-Registration. Brain Topography 22, 307-317.

Zemon, V., Gutowski, W., Horton, T., 1983. Orientational anisotropy in the human visual system: an evoked potential and psychophysical study. International Journal of Neuroscience 19, 259-86.

Figure Legends

Figure 1. Exemplar stimuli. The left column displays examples of phase-shifted (180°) abutting gratings oriented either horizontally (upper row) or vertically (lower row) to induce the perception of either a diamond or circle. The right column displays examples of control stimuli where no illusory forms were induced. Likewise, stimuli varied in their line spacing (1, 2, or 3 cycles/°). Full details of the 18 distinct stimuli used in the study are provided in Materials and Methods.

Figure 2. Schematic of three competing models of illusory contour (IC) sensitivity. For simplicity, only 3 brain regions are illustrated: lower-tier cortices (V1/V2), the lateral occipital cortex (LOC), and parietal cortex. The star in each model indicates the proposed locus of IC sensitivity. Model 1 supports initial IC sensitivity within V1/V2 that is driven by feedforward inputs and/or local lateral interactions. Model 2 supports initial IC sensitivity within the LOC with later effects within V1/V2, though does not preclude IC insensitive influences from parietal cortices. Model 3 proposes that the LOC is sensitive to salient regions of the stimuli and not to the IC itself, though feedback from the LOC is required to effectuate IC sensitivity within V1/V2.

Figure 3. Exemplar group-average VEPs for parietal occipital electrodes PO6 and occipital electrodes OZ. In these plots the red lines represent the illusory contour (IC) stimulus condition and the blue lines the non-illusory contour (NC) stimulus condition. Solid lines refer to the horizontal stimulus condition and the dotted to the vertical stimulus condition. Below each electrode panel a statistical display shows the results of a time-point by time-point repeated measures ANOVA for each electrode ($F_{(1,14)}$; alpha ≤0.05; temporal criterion of at least 11 contiguous time-points).

Figure 4. Group-average global field power (GFP) waveforms conventions for the plots are identical to those in Figure 3. The bottom panel displays the results of a time-point by time-point repeated measures ANOVA on the GFP ($F_{(1,14)}$; alpha ≤0.05; temporal criterion of at least 11 contiguous timepoints).

Figure 5. Statistical analyses of source estimations over the initial 200ms post-stimulus interval. The upper panel displays a time-point by time-point repeated measures ANOVA on the source estimations ($F_{(1,14)}$; alpha ≤0.01; temporal criterion of at least 11 contiguous time-points and spatial extent criterion of 15 contiguous solution points). The red color represents the main effect of stimulus orientation and the blue color represents the main effect of stimulus condition. The bottom panel displays the distribution of significant effects at an exemplar instant (left and bottom panel: the main effect of stimulus orientation at 66ms; right and bottom panel: the main effect of stimulus condition at 100ms).

Figure 6. Statistical analyses of source estimations over the 200-400ms post-stimulus interval. The upper panel displays a time-point by time-point repeated measures ANOVA on the source estimations ($F_{(1,14)}$; alpha ≤0.01; temporal criterion of at least 11 contiguous time-points and spatial extent criterion of 15 contiguous solution points). The red color represents the main effect of stimulus orientation and the blue color represents the main effect of stimulus condition. The bottom panel displays the distribution of significant effects at an exemplar instant (the main effect of stimulus condition at 306ms).

Figure 1

Illusion Present
Illusion Absent
Horizontal Condition
Vertical Condition
Frequency : 1 Cycle /°
Frequency : 3 Cycle /°

Figure 2

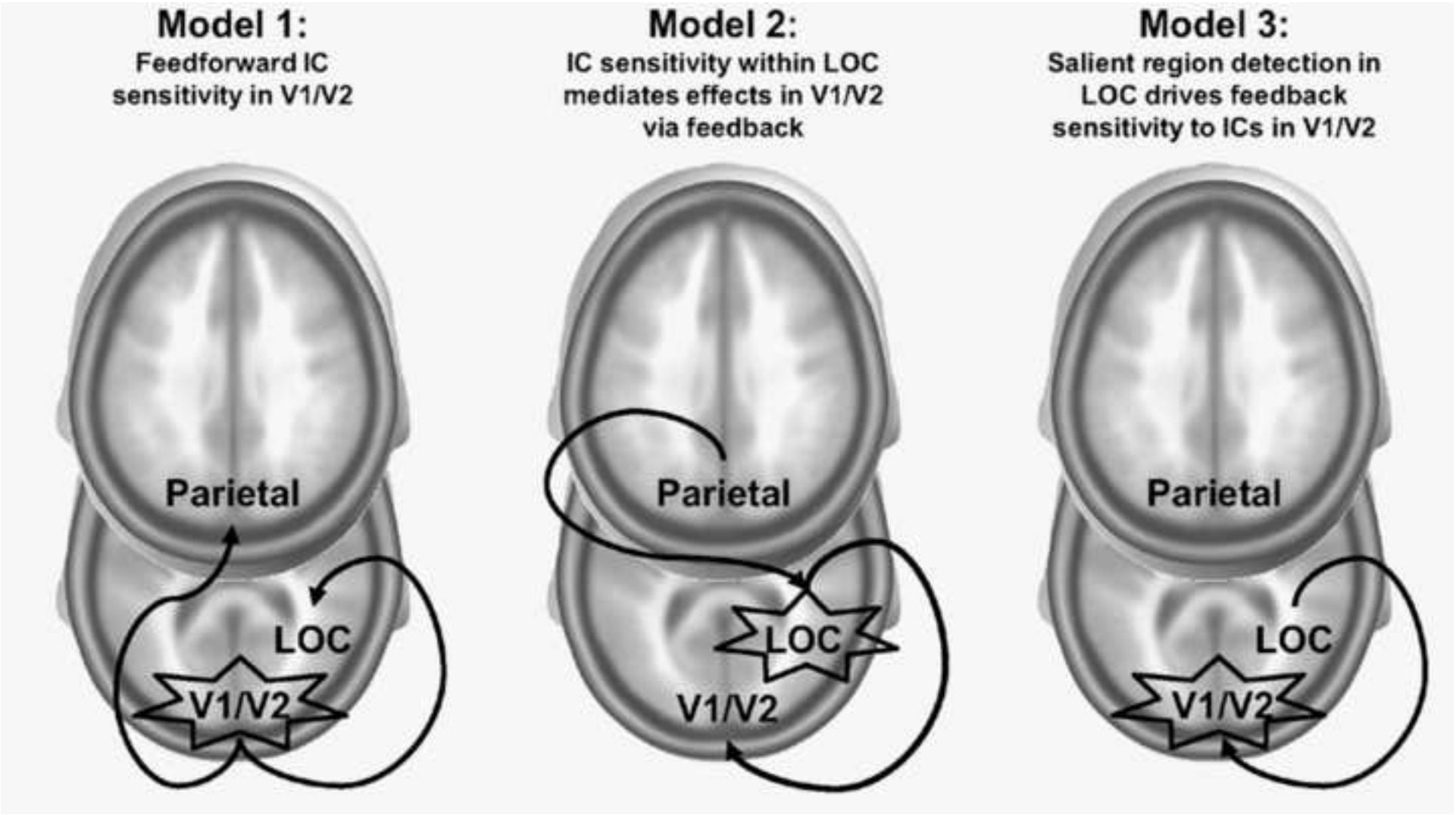
Model 1:
Feedforward IC sensitivity in V1/V2
Parietal
LOC
V1/V2
Model 2:
IC sensitivity within LOC mediates effects in V1/V2 via feedback
Parietal
LOC
V1/V2
Model 3:
Salient region detection in LOC drives feedback sensitivity to ICs in V1/V2
Parietal
LOC
V1/V2

Figure 3

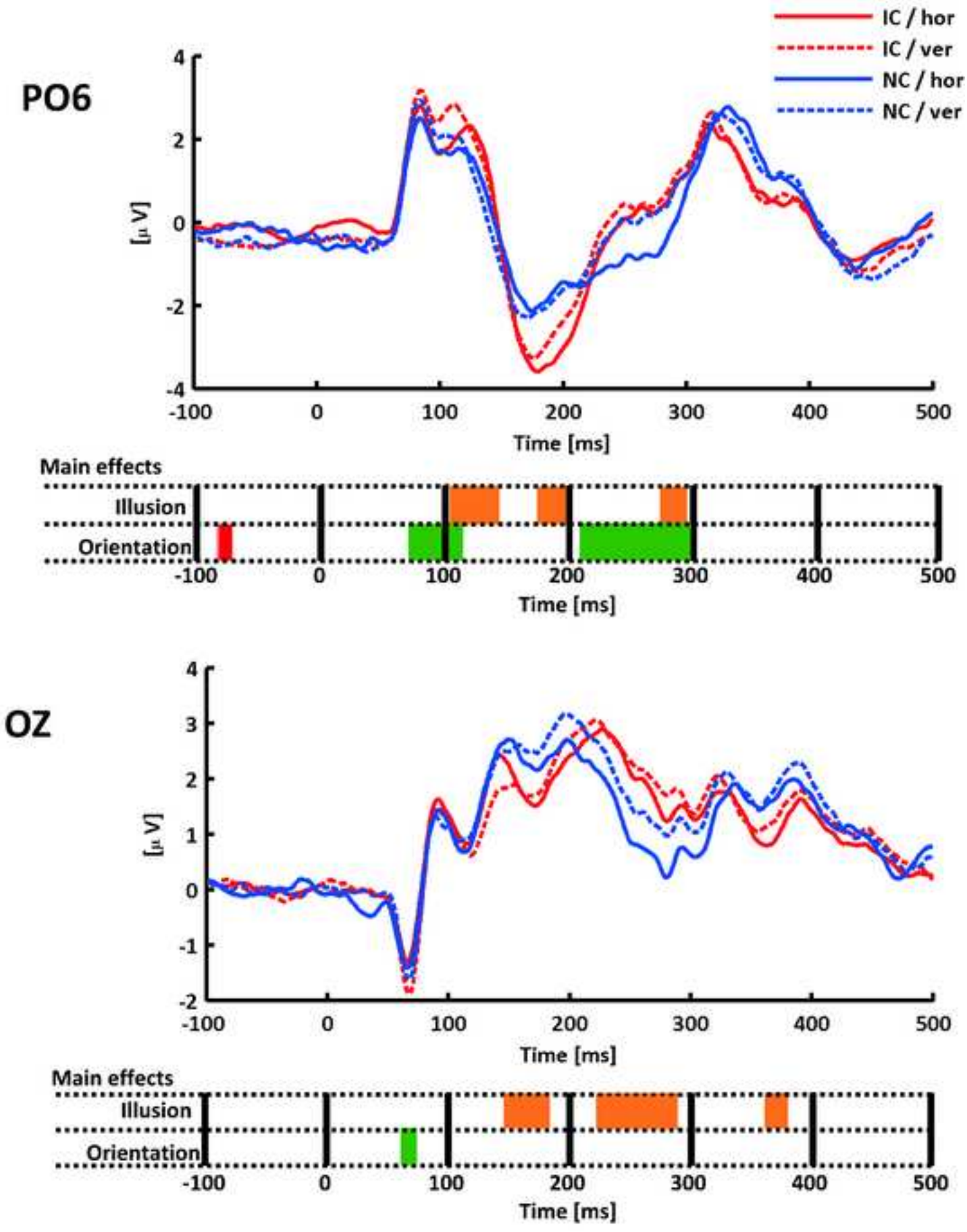
PO6
IC / hor
IC / ver
NC / hor
NC / ver
[μ V]
Time [ms]
Main effects
Illusion
Orientation
OZ
[μ V]
Time [ms]
Main effects
Illusion
Orientation
Time [ms]

Figure 4

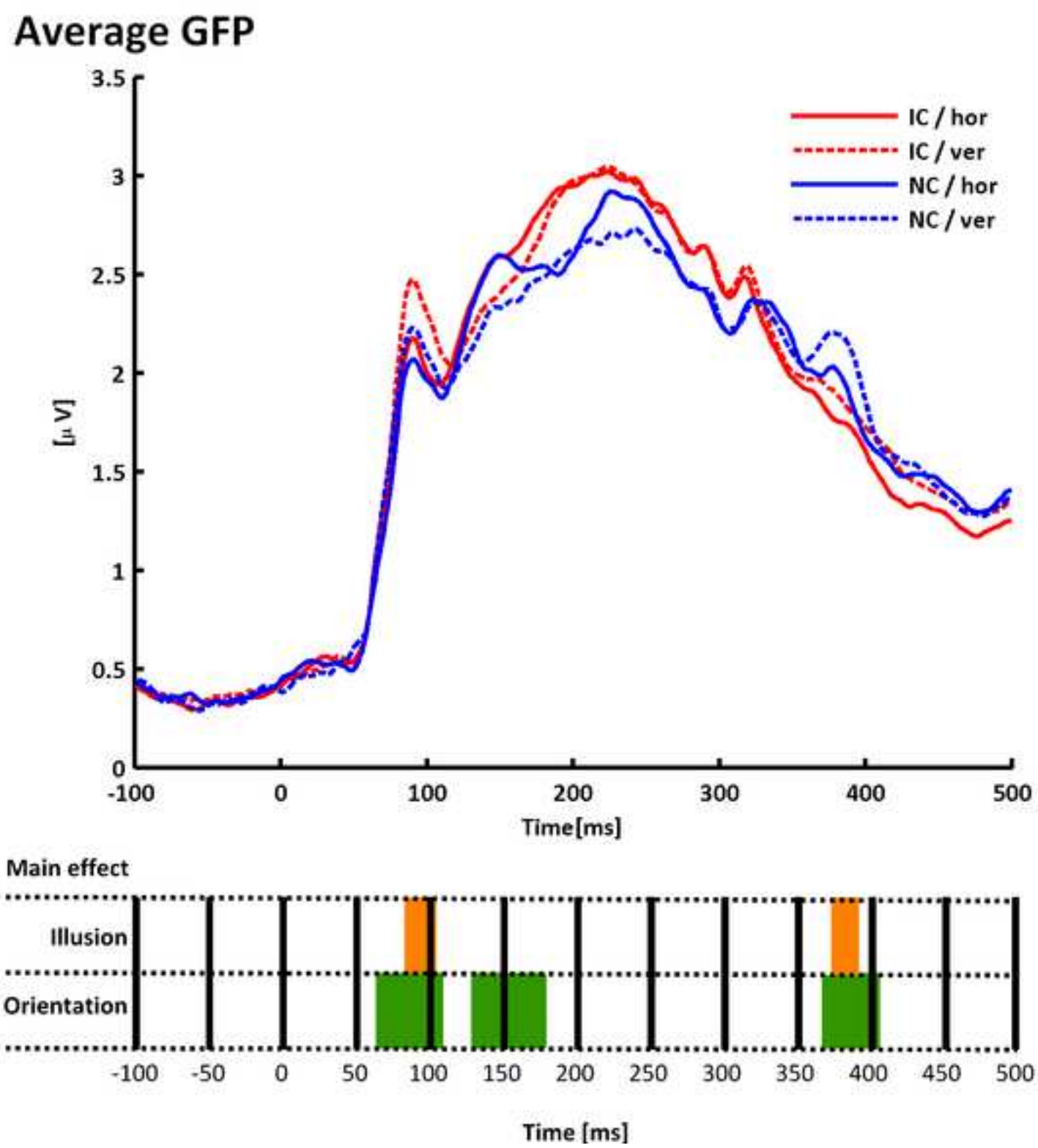
Average GFP
IC / hor
IC / ver
NC / hor
NC / ver
[μ V]
Time[ms]
Main effect
Illusion
Orientation
Time [ms]

Figure 5

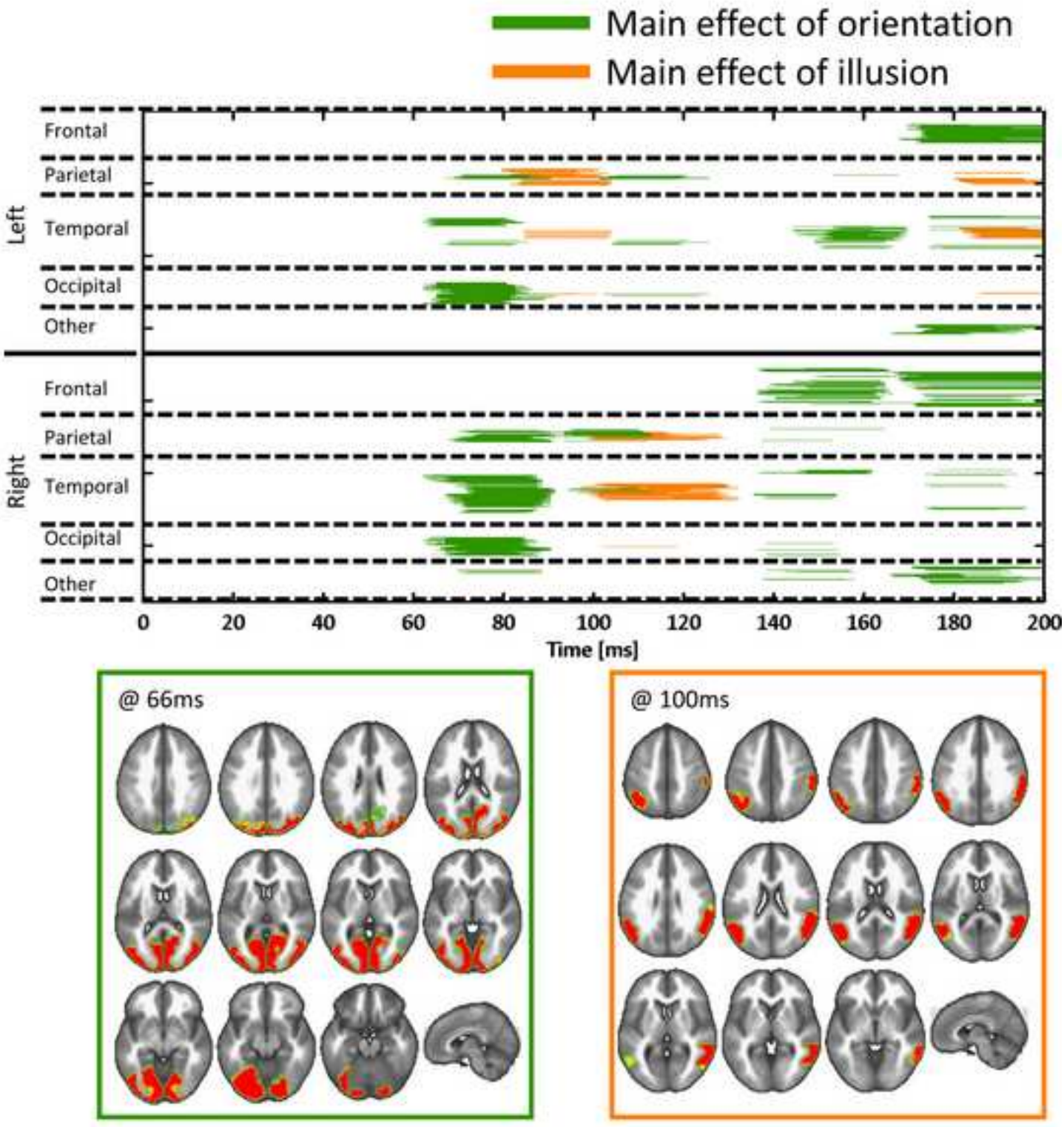
Main effect of orientation
Main effect of illusion
Left
Right
Frontal
Parietal
Temporal
Occipital
Other
0
20
40
60
80
100
120
140
160
180
200
Time [ms]
@ 66ms
@ 100ms

Figure 6

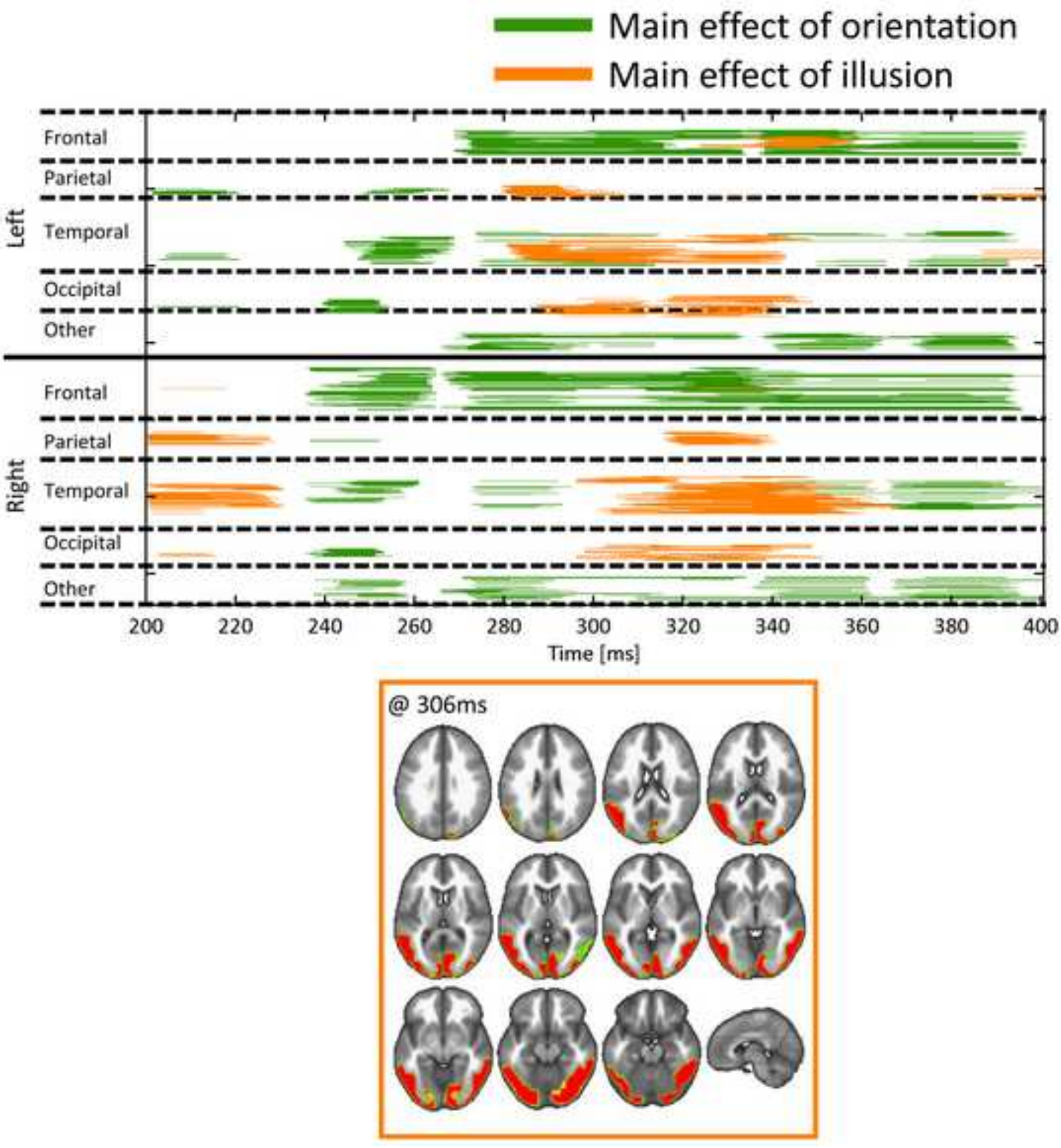
Main effect of orientation
Main effect of illusion
Left
Frontal
Parietal
Temporal
Occipital
Other
Right
Frontal
Parietal
Temporal
Occipital
Other
200
220
240
260
280
300
320
340
360
380
400
Time [ms]
@ 306ms